Analysis of Synchronization Requirements for Integrated Access Backhaul in 5G Networks

Pedro Bemerguy
Federal University of Pará
Belém, Pará
pedro.bemerguy@itec.ufpa.br

Igor Freire
Federal University of Pará
Belém, Pará
igorfreire@ufpa.br

Aldebaro Klautau
Federal University of Pará
Belém, Pará
aldebaro@ufpa.br

Abstract

Integrated Access Backhaul (IAB) is an alternative to decrease the cost of 5G deployments. Nevertheless, the IAB imposes the carrier frequency and time synchronization to be implemented over-the-air (OTA), which have strict requirements for scenarios with multiple-input multiple-output (MIMO), carrier aggregation (CA) and Time Division Duplex (TDD). This work analyzes time and frequency synchronization in an IAB architecture using algorithms that estimate only timing and carrier frequency offset (CFO). Simulation results show that the CFO and TDD time offset (TO) requirements are attended in all SNR cases. However, for CA and MIMO, the requirements are met only when SNR ≥ 8 dB.

1 Introduction

The increase in demand for data-traffic imposes a necessity for radio access network densification. Such a scenario using street-site deployments with fiber communication involves high capital and operational costs [Ron20]. As an alternative to lower these expenses, on the Release 16 [3gpp20], the 3GPP standardized the Integrated Access Backhaul (IAB) following a tree topology hierarchy, with one IAB donor connecting with multiples IAB nodes, where the IAB donor is the only with direct access for 5G core-network [Ron20]. Such deployment imposes that these IAB nodes act as relay nodes to extend the reach of the IAB donor. For it, the IAB node uses over-the-air (OTA) communication to exchange backhaul data, to synchronize with its IAB donor, and to provide wireless access to UE [Ron20], such as in Fig. 1.

Algorithms for OTA timing synchronization using pilot signals is a well-studied topic [Nas15]. However, most of the works that analyze the IAB architecture assumes perfect OTA synchronization between the IAB donor and node. In similar OTA synchronization scenarios, but for Distributed MIMO, [Rah10, Bal13, Rog14] studies synchronization, with [Rah10] uses data-aided synchronization. Though [Bal13] employs a specific antenna for pilot synchronization and [Rog14] admits a coarse synchronization via a wired connection. Those assumptions are not feasible solutions for an IAB scenario.

Therefore, this work has the intention of analyzing the time and carrier frequency synchronization between the IAB donor and IAB nodes and contrasts with TO and CFO restrictions for IAB. For it, this work implements a timer for time synchronization, where to adjust its counter, it has adopted three algorithms: Minn (MN) [Min03], Van de Beek (VB) [VdB97] and Toumpakaris (TP) [Tou09]. The first two measures the timing and fractional CFO (FCFO), and the latter corrects the integer CFO (ICFO).

The remaining of the manuscript is organized as follows. Section 2 explains the OTA system model. Section 3 presents how to achieve time and carrier frequency synchronization. Finnaly, Section 4 and 5 show the simulation results and conclusions, respectively.

2 Over-the-air System Model

Considers a scenario where the IAB system reflects a tree topology, with the parent node being the IAB donor (D_1) and the K child nodes representing the IAB nodes: (C_1, ..., C_K). The K IAB nodes are subject to carrier frequency offset (CFO) due to the in-

In: Proceedings of the IV School of Systems and Networks (SSN 2020), Vitória, Brazil, December 14-15, 2020. Published at http://ceur-ws.org

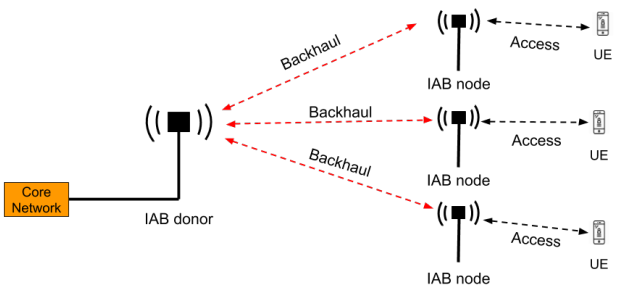

Figure 1: Example of an IAB architecture following a tree topology.

consistent behaviour from the local oscillators of each node when contrasted with the IAB donor local oscillator. This paper denotes the CFOs from K child nodes by $(f^1_{\text{cfo}}, ..., f^K_{\text{cfo}})$. Moreover, there is the spatial distance between the IAB donor and its K child nodes generating a propagation delay (PD) denoted by $(d^1_{\text{dn}}, ..., d^K_{\text{dn}})$.

When the signal arrives at the k-th IAB node, this node applies a downconversion on the received signal based on the carrier frequency produced by its oscillators of $f_{cf} + f^k_{cfo}$. Hence, after this procedure, the receiver sees the pilot sequence as:

$$y^k_d[n] = x^k_d[n - d^k_{\text{dn}}]e^{-j2\pi f^k_{\text{cfo}} \frac{n}{F_s} + \phi_k[n]} + n_k[n], \quad (1)$$

where $n_k[n] \sim \mathbb{CN}(\mu, \sigma^2)$ express the additive white gaussian noise (AWGN) with mean μ and variance σ^2. Lastly, $\phi_k[n]$ is the oscillator phase noise that has two components: a random walk noise on the frequency and phase domain [Zuc05].

3 Time and Carrier Frequency Synchronization

To achieve time synchronization, the IAB donor and each IAB node use a timer to provide the same time notion. However, the timer from each one does not start at the same time, and the timer frequency generated by each local oscillator is not equal. These two combinations produce a time offset (TO) as:

$$\tau_k(t) = \tau^0_k + 2\pi f_t t + \phi(t), \quad (2)$$

where the $\tau_k(t)$ denotes the TO for k-th IAB node, τ^0_k is the initial time offset due to instant where the timer initializes, f_t is the timer frequency offset, and $\phi(t)$ is the noise term equivalent to $\phi[n]$ on (1). To compensate these TO components, a pilot exchange mechanism is necessary to estimate the TO and the CFO. Under the next paragraphs, the $(\tau_1, ..., \tau_K)$ represents the TO for the K IAB nodes.

Fig. 2 describes the pilot exchange mechanism between the IAB donor and the k-th IAB node. At the IAB donor side, its timer counts from 0 to synchronization interval, and in every moment where the counter back to zero, the parent node broadcast a pilot signal for all the IAB nodes. However, the k-th child node does not detect the pilot at the arrival moment, due to two extra delay after the downconversion: the buffer delay (BD) and detection delay (DD). The first kind of delay is the time required for the IAB node to storage all the pilot samples essential for the MN and VB algorithms, and the latter is the time needed to detect where the pilot begins on the buffer. Throughout this work $(d^1_{\text{bd}}, ..., d^K_{\text{bd}})$ and $(d^1_{\text{dd}}, ..., d^K_{\text{dd}})$ expresses the buffer delay and detection delay from the K IAB nodes, respectively. Furthermore, the buffer delay does not change over time, as the pilot signal has a fixed duration. Nevertheless, the detection delay can change at every new pilot detection due to the receiver noise.

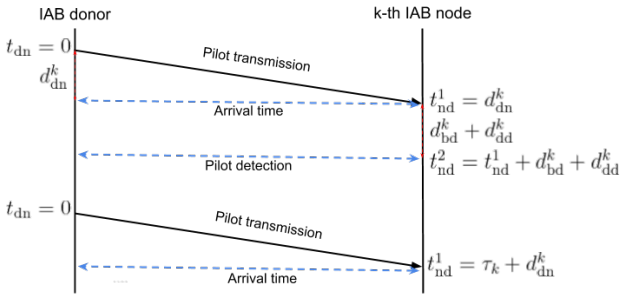

Figure 2: Message exchange mechanism for OTA synchronization using one pilot signal per synchronization interval.

Considering perfect frequency synchronization, at the IAB node, the IAB node starts its counter as zero in every pilot detection, then, the TO from IAB node to the IAB donor is the time it took to detect the pilot signal since the IAB donor sent it: $\tau_k = t^2_{\text{nd}}$, as seen at Fig. 2. To correct this time misalignment, the IAB node needs to adjust its timer by a time advance equal to $t_{\text{adv}} = t^2_{\text{nd}}$. However, the IAB node has only the estimated time advance $(\hat{t}_{\text{adv}})$, which describes t^2_{nd} when the SNR tends to infinity. Under this hypothesis, the MN and VB algorithms estimate the exact beginning sample from the pilot signal all time, meaning the d^k_{bd} and d^k_{dd} does not change. If in scenarios without the infinite SNR the IAB node uses $\hat{t}_{\text{adv}}$ to compensate its initial time offset, then, remaining τ^0_k becomes:

$$\tau^0_k = t_{\text{adv}} - \hat{t}_{\text{adv}}. \quad (3)$$

Nevertheless, perfect frequency synchronization is not realistic. Consequently, the IAB node must use the MN and VB to estimate the fractional CFO, and TP to measure the integer CFO. Based on this two

CFO components, the estimated CFO is defined as $\hat{f}_{\text{cfo}} = f_{\text{icfo}} + f_{\text{fcfo}}$. After each IAB node estimates its CFO, the nodes can find the equivalent timer frequency offset (TFO) based on $\hat{f}_{\text{cfo}}$, considering that the same oscillator generates the timer and carrier frequency. [Rog14] defines the relation between them as:

$$\hat{f}_{\text{tfo}} = \frac{F_t}{F_c}\hat{f}_{\text{cfo}}, \tag{4}$$

where the F_t and F_c are the nominal timer and carrier frequency, respectively. However, there is a remaining error due to the FCFO estimation imprecision by the MN and VB which propagates for the $\hat{f}_{\text{tfo}}$. The error between the true TFO and the $\hat{f}_{\text{tfo}}$ is f_{rto}. Based on f_{rto} and (3), the TO from (2) becomes:

$$\tau_k(t) = t_{\text{adv}} - \hat{t}_{\text{adv}} + 2\pi f_{\text{rto}} t + \phi(t). \tag{5}$$

4 Simulation Results

The simulation follows a tree topology, with 1 IAB donor, $K = 2$ IAB nodes, $d_{pd}^{K} = 800$ m for all nodes. This scenario is similar to the suburban scenario proposed by [Ron20]. Concerning the pilot detection, the simulation uses the TP proposal combining with MN or VB proposal. For the pilot communication, we assume a synchronization interval of 200 ms, with one OFDM symbol per pilot signal. The OFDM symbol duration follows the 5G NR numerology 0, and the OFDM Modulation has a sampling and nominal carrier frequency of 30.72 MHz and 2.5 GHz, respectively. The IAB nodes has an initial oscillator frequency offset of -2000 ppm and +1900 ppm. Finally, the results have an hour of simulation.

Fig. 3 shows the probability density function and the maximum and minimum values for the remaining CFO under different SNR conditions. The results suggests that even in situations of low SNRs, the remaining CFO sustains values within the most restrict CFO requirements for OTA communication, which is ±50 ppb over 1 ms for wide-area communication [3gpp20]. Moreover, the VB performs better CFO estimation than the MN algorithm in all SNR cases.

Analyzing the TO requirements for some IAB applications [3gpp20], the MN and VB meet the TO specifications for TDD applications (± 1.5 μs), but for intra-band contiguous CA (± 260 ns) and MIMO (± 32.5 ns), only the MN can provide time synchronization when SNR ≥ 8 dB, as seen in Fig. 4. One of the reasons for the MN performs better than the VB for TO; it is the MN advantage of using all the OFDM symbol from the pilot signal, where the VB uses only the CP samples. The OFDM symbol duration is greater than the CP duration, so there are more samples to mitigate the channel noise effects.

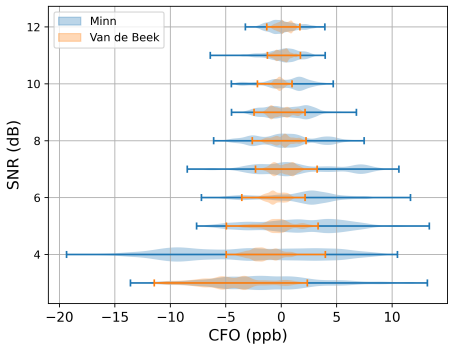

Figure 3: Compares the probability density function for the remaining CFO under different SNR cases using the MN and VB algorithms for pilot detection.

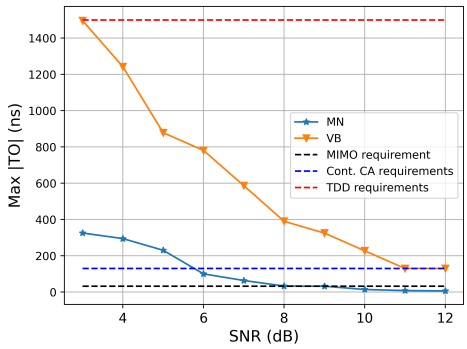

Figure 4: Compares the timer time offset using the MN and VB algorithms for pilot detection with the time synchronization requirements for TDD, CA and MIMO.

5 Conclusion

This paper introduced a study to estimate the CFO and TO in IAB scenario using the TP, MN and VB algorithms for pilot detection. Moreover, this work simulates an IAB architecture similar to [Ron20]. The results show that the VB and MN meet the CFO requirements for an IAB scenario, with VB performing better CFO estimation than the MN. However, only the MN meets the TO requirements for CA and MIMO when the SNR ≥ 8 dB. For TDD applications, both algorithms attend the TO specs.

References

[Ron20] H. Ronkainen, et al, "Introducing integrated and access backhaul", Ericsson, July 2020.

[3gpp20] 3GPP, "Integrated access and backhaul radio transmission and reception", Jun. 2020.

[Nas15] A. A. Nasir, et al, "Timing and carrier synchronization in wireless communication systems: a survey and classification of research in the last 5 years", EURASIP Journal on Wireless Comm.. and Networking, vol. 2016, Jul. 2015.

[Rah10] H. Rahul, et al, "SourceSync: A Distributed Wireless Architecture for Exploiting Sender Diversity", ACM SIGCOMM, Aug. 2010.

[Bal13] H. V. Balan, et al, "AirSync: Enabling Distributed Multiuser MIMO with Full Spatial Multiplexing", IEEE Trans. on Networking, vol. 21, no. 6, pp. 1681-1695, Dec. 2013.

[Rog14] R. Rogalin, et al, "Scalable Synchronization and Reciprocity Calibration for Distributed Multiuser MIMO", IEEE Trans. on Wireless Comm., vol. 13, no. 4, pp. 1815-1831, Apr. 2014.

[Min03] H. Minn, et al, "A Robust Timing and Frequency Synchronization for OFDM Systems", IEEE Trans. on Wireless Comm., vol. 2, no. 4, Jul. 2003.

[VdB97] J. van de Beek, et al, "ML Estimation of Time and Frequency Offset in OFDM Systems", IEEE Trans. on Signal Proc., vol. 45, no. 7, Jul. 1997.

[Tou09] D. Toumpakaris, et al, "Estimation of Integer Carrier Frequency Offset in OFDM Systems Based on the Maximum Likelihood Principle", IEEE Trans. on Broadcasting, vol. 55, no. 1, Mar. 2009.

[Zuc05] C. Zucca, et al, "The Clock Model and Its Relationship with the Allan and Related Variances", IEEE Trans. on Ultras., Ferro. and Freq. Control, vol. 52, no. 2, Feb. 2005.